Engineering and Technology Journal
Journal homepage: https://etj.uotechnology.edu.iq

An Unbalance Three Phase Currents Detection Technique for Load Side Broken Conductor Fault in the Iraqi Distribution System

Ali G. Al-Baghdadi[a]*, Mohammed K. Abd[a], Firas M. F. Flaih[b]

[a] Electrical Engineering Dept., University of Technology-Iraq, Alsina'a street, 10066 Baghdad, Iraq.
[b] State Company of North Distribution Electricity, Iraq.
*Corresponding author Email: eee.19.33@grad.uotechnology.edu.iq

HIGHLIGHTS

- Design of a MATLAB model capable of simulating the real distribution 11kv feeder.
- The over-current relay is completely not sensitive to LSBC, and the neutral current fault relay is only sensitive to (0-70) % of the feeders.
- Using the unbalanced current method, 87% - 93% of feeders can be protected.
- Use mathematical methods to analyze LSBC fault.
- A comparison between the suggested approach with current research is written.

ARTICLE INFO

Handling editor: Ivan A. Hashim

Keywords:
Broken conductor faults; Single Line-to-Grounc faults; unbalanced 3-ph voltage; Unbalanced 3-pł current; High impedance fault.

ABSTRACT

Electrical supply safety and quality represent targets that Iraqi power distribution companies always strive to meet. Load-side broken conductor fault LSBC is one of the greatest faults affecting both targets. Stand out since the magnitudes of the impact on the system are too small to activate the relevant system protection devices in Iraqi substation 33/11kV. Therefore, protection from LSBC faults has been one of the biggest challenges in the Iraqi electrical distribution system. In this context, the main aim of this article is to present a method for detecting LSBC faults by unbalanced three-phase currents faults measured in a 33/11kv distribution substation. Using computer simulations based on an actual distribution 11kV feeder model, this method was qualitatively tested. Then, a relationship between mathematical and simulation results was made. Finally, A comparison of the proposed method and recent literature was written. According to the obtained results of case studies, the protection devices in the Iraqi substations cannot efficiently sense the LSBC fault. The overcurrent relay is completely not sensitive to LSBC, and the neutral current fault relay is only sensitive (0-70)% of the different types of feeders under the study. While the proposed unbalance, the current method had been detected with 87% -93% of 11 kV feeders. The proposed techniques are applicable and compatible with the existing traditional protection of the overcurrent and earth fault protection system in the Iraqi 33/11kV substation.

1. Introduction

1.1 General Context

An open phase detection (OPD) system's main job is to dependably protect against imbalances that might negatively affect important safety features, harm significant capital investments, or stop plant operations. An OPD system must also provide adequate security against false tripping routine, non-harmful unbalance conditions, and momentary or short-lived transient unbalance conditions [1]. The open conductor and open phase conditions occur when a power network conductor is lost because of a blown fuse, incorrect switching operation, unintentionally grounded conductors, loose connections, or a broken conductor state, as shown in Figure 1. It contains two ends, the first towards the loads and the second towards the source. There is no current flowing behind the open conductor terminal in a broken conductor condition described by unbalanced voltages, lowered current in the circuit, and low fault or ground current [2]. Overhead broken or downed wires cause distribution networks problems that might be difficult to detect. Traditional detection approaches have relied on some zero current sequence detection, but this limits the fault path's impedance and the protection device's sensitivity to this type of fault detection.

http://doi.org/10.30684/etj.2022.135940.1291
Received 15 September 2022; Accepted 13 November 2022; Available online 30 December 2022
2412-0758/University of Technology-Iraq, Baghdad, Iraq

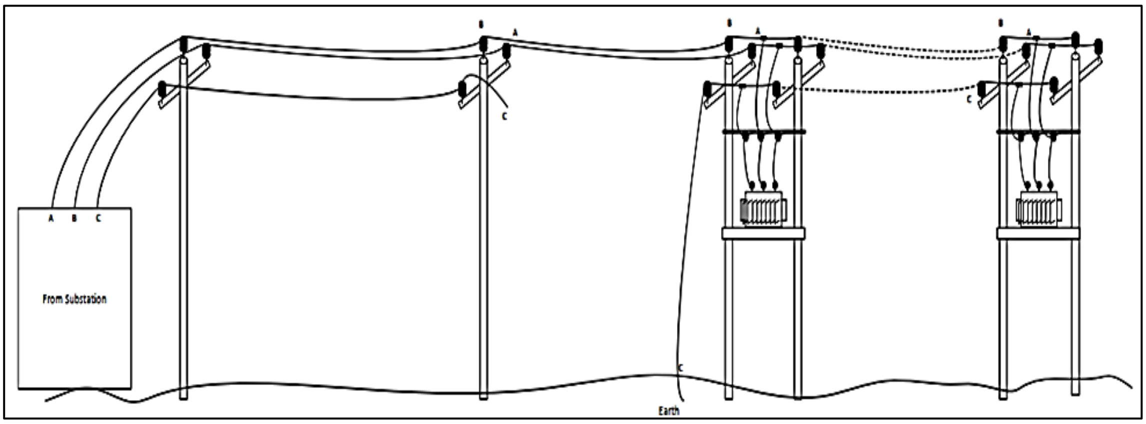

Figure 1: Broken conductor fault in the distribution system

Modern multifunction protection relays can do more detailed measurements, such as negative sequence current detection, which has been included in certain intelligent electronic products to detect broken conductors. However, several issues restrict the efficacy of this approach. Thus, it is not a foolproof way of detection. Suppose the broken conductor has a high impedance on the source side or contacts the ground on the load side with any impedance. The current result could be insufficient to enable the protection distribution system [3]. In a medium voltage distribution system, broken conductor detection protection shows an open phase state on the circuit.

Broken conductor faults occur mostly in the distribution systems. When a primary electrical conductor breaks and makes unwanted contact with the earth, the fault current drawn may be very high if a low-impedance fault object is found. Consequently, overcurrent protection in the Iraqi sub-station (33/11) kV will work if the values of currents are more than 300A. But a problem facing the electrical engineer in 11kV feeders of Iraqi distribution networks is the ground fault (single line to ground) in the feeder, which occurs at LSBC fault without circuit breaker trips and protection relay with remains the feeder in CLOSE position (ON, working status). The current value in this type of ground fault is a few, and the relays will not sense this value as it is set to (30 A). Therefore, it may lead to damage and ensure service continuity and personnel safety. Therefore, studying and analyzing this type of fault is very important. Because of the challenges experienced previously, this article recommends that traditional methodologies based on unbalanced current faults measured at a substation be used. The result indicated that the method suggested in this study is both easier and more cost-effective than the other methods. Therefore, the contributions of this paper are:

- Design of a MATLAB model capable of simulating the real distribution 11kv feeder of the conductor break.
- Use the conventual economic method, one measurement from one side of a feeder in the substation to detect the LSBC fault, which is practical in real-world distribution systems.
- Protect the feeder 87% from LSBC fault.

The paper is organized into five sections. Section 1 presents the introduction to the topic. Section 2 details the research methodology, including a detailed description of mathematical analyses of the LSBC fault. Also, case study, procedures to represent the feeder 11kv in MATLAB simulation, and Simulink design. Section 3 provides test results of software simulation. Section 4 presents the discussion and comparison between the proposed method's results and its counterparts. Finally, section 5 of the paper presents the conclusion and research suggestions for future work.

1.2 Literature Review

This subsection aims to review the literature on broken conductor faults (BCF), including methodologies for its detection. There are four types of BCF detection methods in the distribution system: Conventional, signal processing, mathematical, and artificial intelligence. In [4], communications networks enable BCF detection. This paper focuses on wireless communications within a privately owned network and the exchange of information between assets, such as intelligent electronic devices and substations. It should be noted, however, that using communication-based methods increases the hardware and software complexity and is not low cost. A similar approach was used in [5], the broken feeder detection is carried out using smart grid infrastructure (available communication system), and the given detection method is based on measurements taken on the load transformers' low voltage side. Without adding voltage transformers, the suggested technology identifies such faults by simply monitoring the magnitude of the recorded three-phase voltage at the load side. A strong threshold value is recommended to provide dependability under all fault scenarios and security against normal imbalance.

Because power incorporates the properties of both voltage and current, [6] studies the idea of utilizing power to diagnose BCF. After a single BCF breakdown, the authors thoroughly examine the electrical properties of both sides of the transformer. On the low-voltage side, the fault-phase corresponding to the winding's active and reactive power is near zero. But this method remains successful only in all types of power plants and substations and is not tested on the distribution system. [7], considers the relationship between I_2 and I_0 with the I_1 during a broken conductor occurrence and suggests an asymmetric current method. The I_2/I_1 and I_0/I_1 relationships may be utilized to discover rapid grid variations that could be produced by a single-phase failure using this approach. However, the results highlight scenarios where the methodology cannot be applied. Those drawbacks mainly relate to the delta transforms placed downstream on the relay's position.

In [8], this research compares the efficiency of Negative Sequence Voltage (NSV) applied to the detection and differentiation of conductor breaks to other voltage disturbances and switching that typically occur in the distribution system. The post-fault value for the conductor break was much greater than for the other events, with an average value of 78,92 V and a maximum value of 90,28 V for the other occurrences. However, faults at the feeder's end or inside branches are less likely to be detected, and the BCF detection condition changes depending on the resistance and fault location. As a result, NSV sensitivity varies with these variables. In [9], The absence of unusual detectable voltage and current responses when a conductor is open, according to the authors, is due to the supply voltage's positive sequence character. On the other hand, an open conductor would provide unique voltage and current responses if the source voltage was in zero sequences. Therefore, the key idea of the proposed scheme is to use the zero-sequence component for open conductor detection. Based on this understanding, a relaying scheme that uses the 3rd harmonic power is proposed to solve the open conductor detection problem. In [10], a method for identifying open conductor breakdowns were presented in power distribution networks using DGs. The suggested technique is based on measurements taken by the feeder remote terminal unit (RTU), which is used to operate a smart power distribution network. Feeder RTUs are placed in the protection system, remote control switches, and other controllers to secure and monitor the distribution system. On the other hand, as the number of DGs connected to the network expands, the holding voltage at the load side of the open conductor point remains near normal, making problems in individual RTUs impossible to detect.

A broken Conductor (BC) type of High Impedance Fault (HIF) occurs in the distribution system. So, in [11], a methodology for detecting HIF generated by cable breakage is presented. The algorithm is based on the analysis of the harmonic and the variation of the system currents' positive and negative sequence components. The method is based on the frequency domain. It is worth pointing out that this algorithm works in three-phase networks with grounded neutral in the substation. Unfortunately, the broken cable detector algorithm does not cover all cases. There may be exceptions where a wire opening does not cause unbalance, and the algorithm does not act.

In [12,], Machine learning ML strategies are used for detecting BCF in smart distribution systems due to their adaptability and effectiveness. The basic idea of machine learning is to parse data, find out from it, and apply what they have discovered to create informed decisions. For instance, in [13], to detect fault taking, recorded data of micro-phasor measurement units through BCF. The voltage signals' frequency component is then chosen as a feature vector. The neighborhood component feature selection approach is used to extract more important features and reduce the feature vector dimension. A support vector machine classifier is then applied to the decreased dimension training data. In [14], a combination of discrete wavelet transforms DWT, and Fuzzy inference system FIS has been proposed for HIF detection. The proposed method uses current signals from one end that are pre-processed using DWT to obtain appropriate input features. Finally, the wavelet-processed features are given to the FIS for fault detection. The proposed method has been validated using both Mamdani and Sugeno-type FIS. However, Machine learning needs initial investment that may contain the communication link, metering measurement, and wireless sensors. Using this equipment in the distribution system is not recommended from an economic factor and complexity.

In the previous studies, there are four forms to the experiment objectives as follows:

1) Detection is the ability to sense the presence or absence of a malfunction by the protection system.
2) Classification: It is the knowledge of the protection system for the type of fault.
3) Location: The next step of protection is to locate the fault by distance or geographical area.
4) Isolation: It is to separate the fault site in the least possible part of the network so that other electrical loads are not affected.

The last three parts (classification, location, Isolation) have been canceled from the current research because they are not applicable in Iraqi substations because of their high costs, unlike the first part, which can be applied directly without cost.

2. Mathematical Analyses of The LSBC Fault

The widely applicable symmetric components transformation (SCT) may be used to perform LSBC fault analysis. Thus, under balanced conditions, all three phases are symmetrical; hence the calculation/analysis of various related parameters is relatively easy. However, suppose a three-phase to the ground, triple line fault, phase-phase, or phase-ground fault occurs. Combined with symmetrical and unsymmetrical faults, the analysis becomes time-consuming and tedious if there is no symmetry. So, the condition is like this: any asymmetrical phase can be expressed as a linear function of the symmetrical phase by using complex transformation with matrices. Generally, these symmetrical components are termed positive, negative, and zero sequence phases. Adopting such a methodology eliminates the interdependence of the equations of one phase to another; hence, the calculations which are supposed to be carried out on one single phase become much more accessible. Figure 2. shows the LSBC fault design, which considers a fault section in the feeder that joins a source side to the loads. It's worth noting that this fault seems more probable to appear in overhead feeders than in cable feeders.

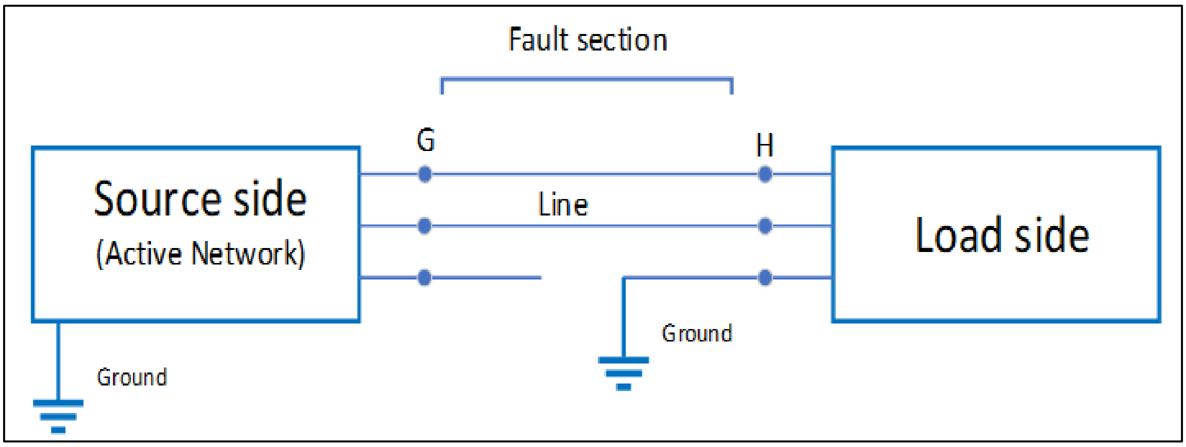

Figure 2: The LSBC fault discretion in the fault section

The widely used symmetric components transformation (SCT) may be used for LSBC fault analysis. It may be used, among other things, to analyze overhead, grounded, or resonant-grounded systems, radial or mesh feeders, passive or active power loads, and more. A sinusoidal condition is considered using the SCT, and phasor algebra is used.

A series impedance ZS is assumed to describe the BCF to establish a generic theory. In addition, as indicated in Figure 3, the conductor-to-ground contact is taken into consideration using the shunt impedance Zg.

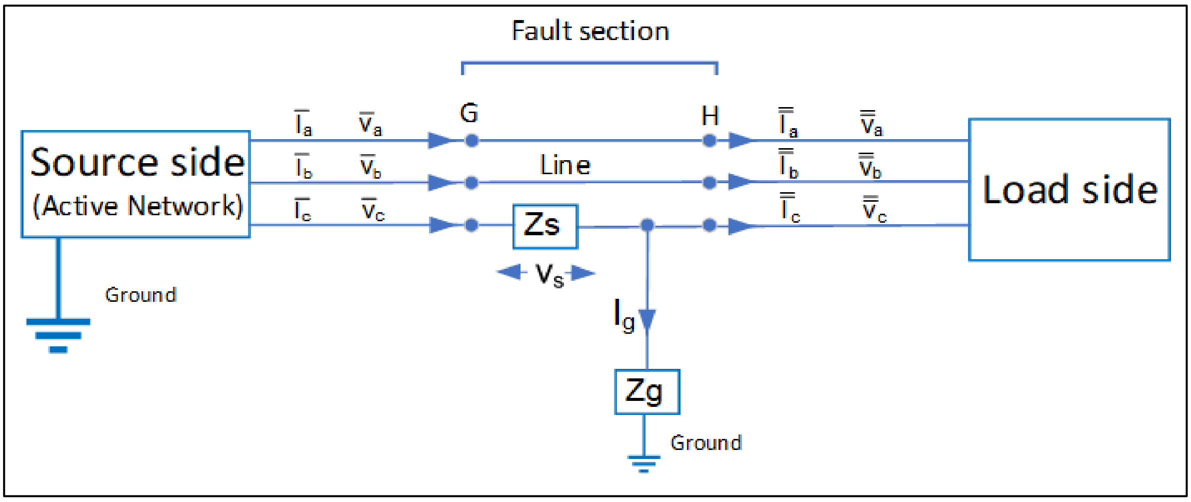

Figure 3: A fault section description

The series impedance goes from infinity Z_S to infinity, and the single line to ground fault connection leads, on the other hand, follows Zg to zero. The SCT is used to investigate the LSBC fault on the G, and H fault sections, as shown in Figure. 3. In section G, the line currents with symmetrical components are as follows [15]:

$$\begin{bmatrix} \bar{I}_{c0} \\ \bar{I}_{c1} \\ \bar{I}_{c2} \end{bmatrix} = \frac{1}{3} \begin{bmatrix} 1 & 1 & 1 \\ 1 & a & a^2 \\ 1 & a^2 & a \end{bmatrix} \begin{bmatrix} \bar{I}_a \\ \bar{I}_b \\ \bar{I}_c \end{bmatrix} \quad (1)$$

Where the subscripts 0, 1, and 2 indicate the zero, positive, and negative sequence components, respectively, and $a = e^{-j2\pi/3}$. In a compact form, Equation (1) becomes the following:

$$\left[\bar{I}_{c012}\right] = \left[F\right]^{-1}\left[\bar{I}_{abc}\right] \quad (2)$$

As a result, section H may be rearranged as follows:

$$\begin{bmatrix} \overline{\overline{I}}_{c0} \\ \overline{\overline{I}}_{c1} \\ \overline{\overline{I}}_{c2} \end{bmatrix} = \frac{1}{3}\begin{bmatrix} 1 & 1 & 1 \\ 1 & a & a^2 \\ 1 & a^2 & a \end{bmatrix}\begin{bmatrix} \overline{\overline{I}}_{a} \\ \overline{\overline{I}}_{b} \\ \overline{\overline{I}}_{c} \end{bmatrix} \tag{3}$$

The next formal may be written for the fault H, G section using Kirchhoff's Popular theory:

$$\begin{bmatrix} \overline{\overline{I}}_{a} \\ \overline{\overline{I}}_{b} \\ \overline{\overline{I}}_{c} \end{bmatrix} = \begin{bmatrix} \overline{I}_{a} \\ \overline{I}_{b} \\ \overline{I}_{c} - I_g \end{bmatrix} \tag{4}$$

Combining (1), (3), and (4) obtained:

$$\begin{bmatrix} I_{g_{c0}} \\ I_{g_{c1}} \\ I_{g_{c2}} \end{bmatrix} = 3\begin{bmatrix} \overline{I}_{c0} - \overline{\overline{I}}_{c0} \\ \overline{I}_{c1} - \overline{\overline{I}}_{c1} \\ \overline{I}_{c2} - \overline{\overline{I}}_{c2} \end{bmatrix} \tag{5}$$

3. Proposed Method

The assumption of balanced three phases is not practical at the medium voltage (11 kV and 33 kV) level, but it is a reasonable approximation [16]. In addition, the studies' stated objectives are to verify that the 11kV circuits' 3-phase currents are balanced under standard operating circumstances [17]. As can be seen, the resultant current unbalances associated with the LSBC fault event can be detected. Thus, this paper proposes the three-phase current unbalance percentage as the LSBC fault detection evaluation index to meet the distribution network's actual protection. The unbalanced percentage of the 3-ph current is the ratio of the difference value between the maximum and minimum current to the maximum value among the three-phase current. The mathematical expression is as follows:

$$I_{unb} = (|I_{max}| - |I_{min}|) / |I_{max}| \times 100\ \% \tag{6}$$

In the formula, $|I_{max}|$ is the maximum value among the three-phase current, and $|I_{min}|$ is the minimum value among the three-phase current [18]. Three categories may be used to categorize imbalanced terminology: unbalanced harmonic disturbances, unbalanced fundamental amplitude unbalances, and unbalanced fundamental phase difference unbalances. The occurrence of at least one of these features is enough for a distribution network to become unbalanced [19].

In Figure 4, the scheme begins by entering three phases (Ia, Ib, and Ic) to start the comparison with the maximum current of the three phases' electrical network is 300 amperes. However, most of the faults are from series, and parallel types, high values of current occur that exceed the permissible limit of 300 amperes, which leads to over-current relay operation. At the same time, another conventional protection device is a neutral current relay, which protects from earth fault current at limits between (30 -150) A. The third stage is the proposed technique for detection of LSBC faults by unbalanced currents in which the percentage of unbalanced currents is greater than 10%. However, the disadvantage of this method is that it is unsuccessful when the LSBC fault is far from the substation. But its advantage is that it is less expensive than other methods, and can be applied directly to Iraqi substations.

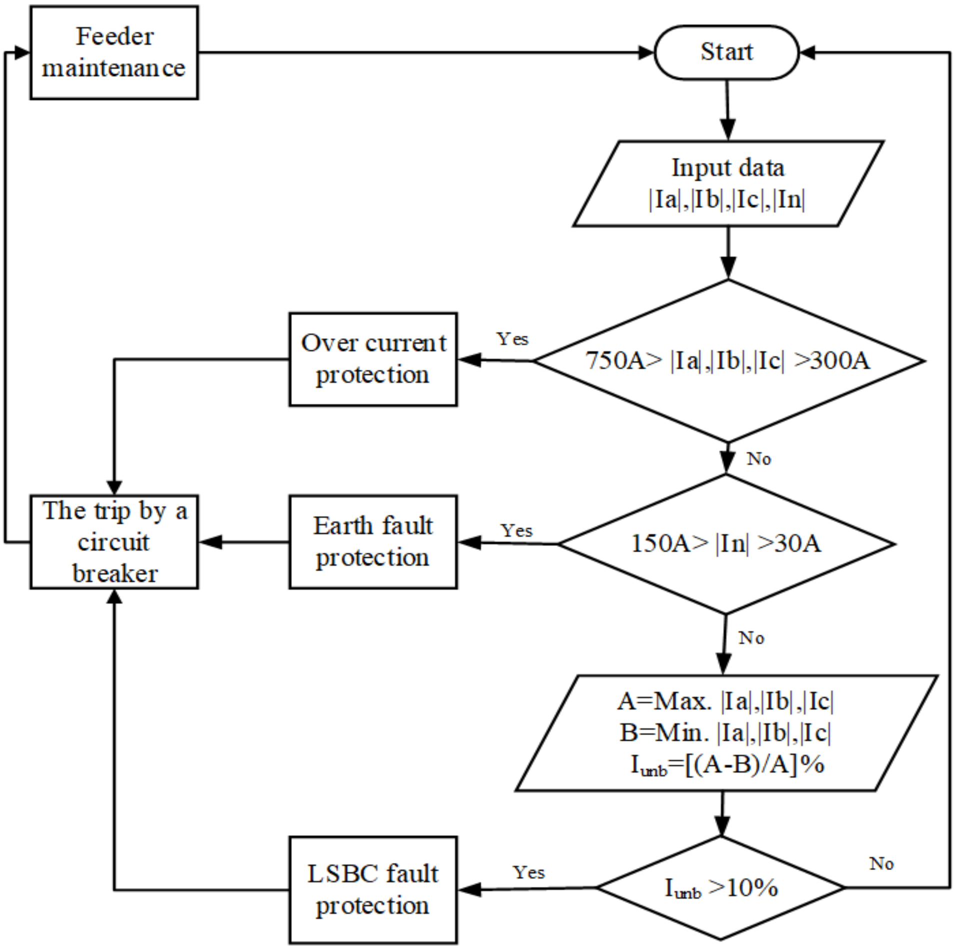

Figure 4: The flow chart of the unbalance fault detection

So, in this study, the absolute or r.m.s values to 3-phase currents are considered unbalanced.
In the Iraqi distribution network, the most conventional primary enabled protection limits for 11 kV feeders are [20] [21]:

$S = \sqrt{3}\, V\, I$

$31.5\text{MVA} = \sqrt{3} \times 11\text{kV} \times I$

$I = 1653$ Amper

Feeder numbers to one power transformer =7

The current for one 11kV feeder =1653 / 7=236 A

Low over Current Setting = Feeder Load Current × Relay setting = 236 A X 125% =295 A ≃ 300A = I_{max}

$$\text{Overcurrent (Low), which is } I_{max} = 300 \text{ A.} \tag{7}$$

$$\text{Overcurrent (High), } I_{max} \times 250\% = 750 \text{ A.} \tag{8}$$

$$\text{Earth fault (High), which is } I_{max} \times 50\% = 150 \text{ A.} \tag{9}$$

$$\text{Earth fault (Low), } I_{max} \times 10\% = 30 \text{ A.} \tag{10}$$

Where I_{max} is the maximum phase current.

4. Simulink Design

Al-Abasia substation in the Najaf area comprises 33/11 kV power transformers with a power rating of 31.5 MVA. Two feeders are at the 33kV level feed for 33/11 kV substations. Twelve 11kV feeders outgoing from Al-Abasia station serve a sizeable mixed residential, government, and agriculture loads. Therefore, only four 11kV feeder will be understudied, named (f_1, f_2, f_3, f_4), as shown in Figure 5 where f_4 was represented.

This system is composed of 63-line sections and 64 buses. All line sections between buses (1 to 64) are selected for this study. The MATLAB simulation software was used to model a realistic distribution 11kv feeder shown in Figure 6.

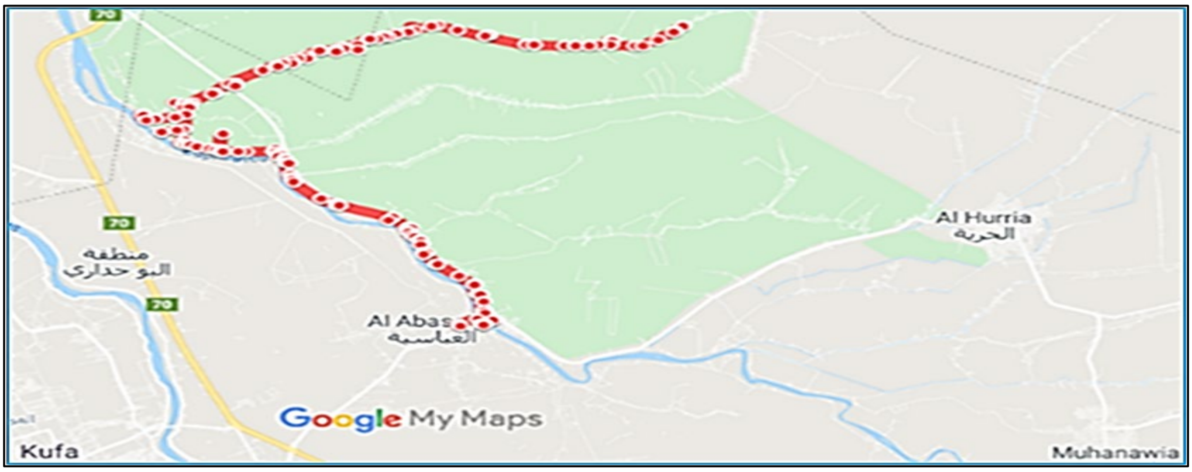

Figure 5: f_4 - feeder 11kV

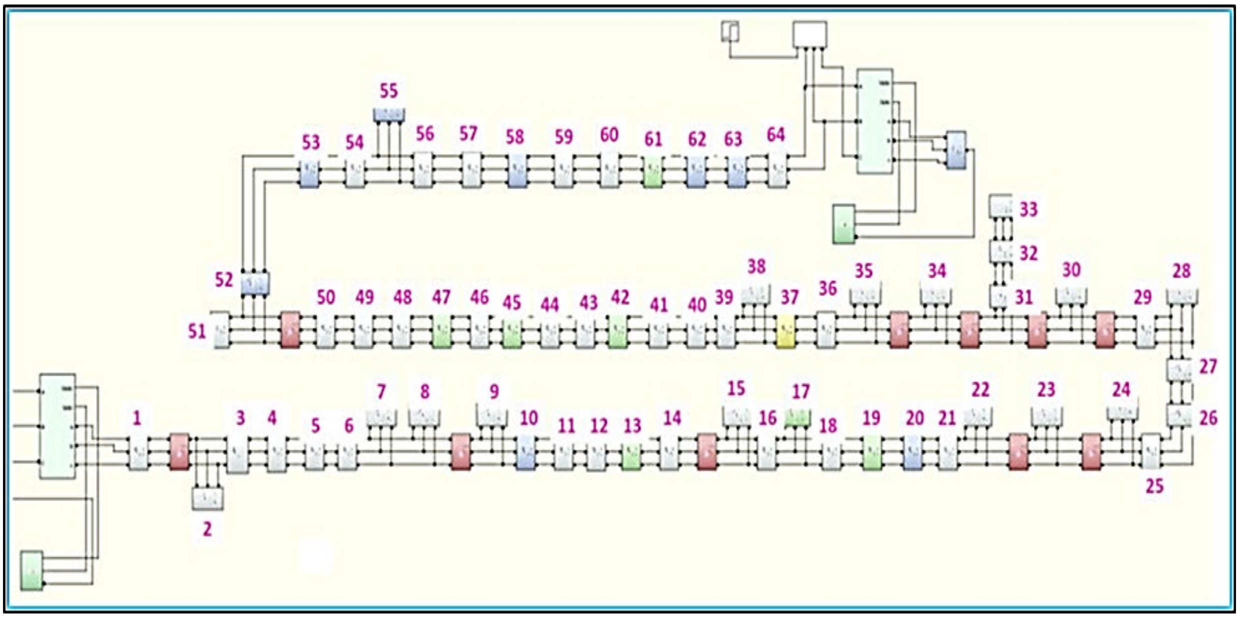

Figure 6: The feeder f_4 Simulink block

4.1 Procedures to Represent The Feeder 11kv in MATLAB Simulation

Choose feeder 11kv (f_1, f_2, f_3, f_4) for a case study, as shown in Table 1. The first column (No.) in Table 1 represents the numbering of the 11Kv feeders inside Al-Abasia substation, from which f_1, f_2, f_3, and f_4 were chosen as a case study for the current research paper. The second column (Feeder name) represents the name of the residential or agricultural area fed by the feeders. Also, the third column (Loads kW) represents the load of each feeder.

Table 1: Outgoing 11kV substation feeders

Al–Abasia substation (33/11) kV/2*31.5 MVA		
Feeder No.	**Feeder name**	**Loads kW**
f_1	Al-Tawari	1420
f_2	Madina 1	2710
f_3	Madina 2	4210
f_4	Al-Haidari	6140
f_5	Al-Bidir	1123
f_6	Al-Faris	5230
f_7	Madina 3	3210
f_8	Al-Taabw	900
f_9	Abu Gharib	2240
f_{10}	Al-Wahabi	1230

GPS (Global positioning system) points are taken for each angle of the feeder 11kv by a GPS device Figure 7.

Figure 7: GPS device used to measure section distance of feeder [22]

All the information is recorded in the datasheet. As an example, the table in the appendix represents all the data for the f_{10} feeder that feeds Al-Wahabi village in Najaf governorate, where it is written by a working team that surveys the f_{10} in the field with the help of GPS. Through this table, data can be entered into various distribution network simulation programs such as MATLAB, Cymdist, etc, as shown in Figure 8.

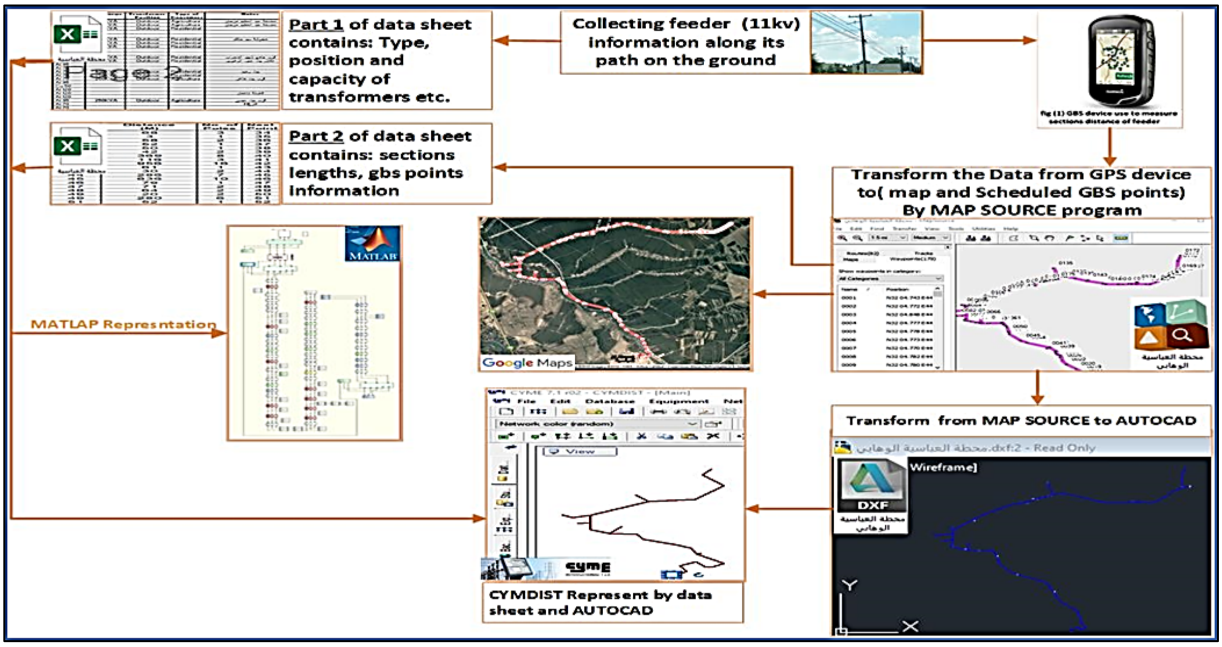

Figure 8: The Block diagram explains how to represent an 11kv feeder

The 11KV feeder can also be represented in the CYMDIST program after converting the data in the GPS device to the personal computer using the Map Source program and then transferred to the AUTOCAD program and from there to the **C**YMDIST program, as shown in Figure 8. The feeder can also be represented on a Google Map by directly converting the data from the Map Source program to a Google Map.

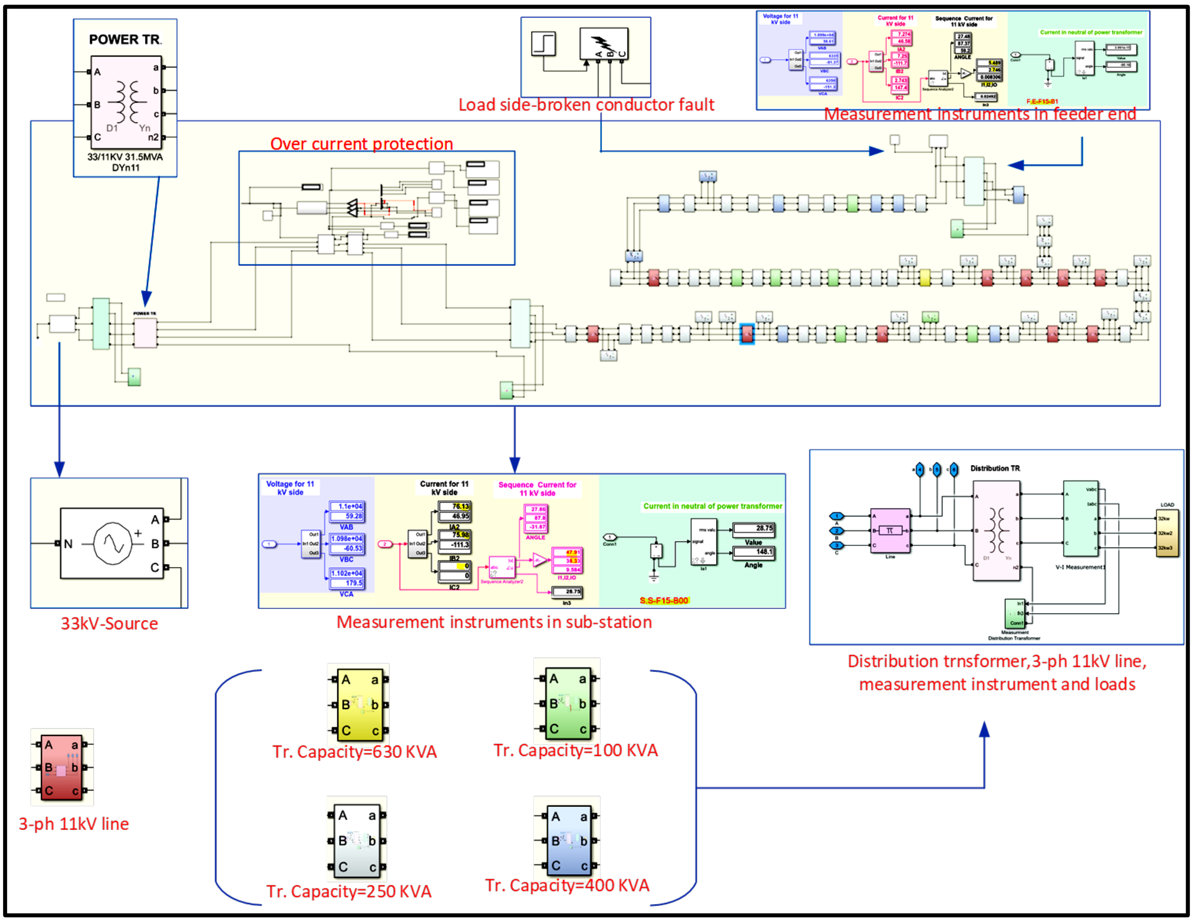

Figure 9: Simulink design to f_4

The final stage is Simulink design, where the four feeders under study are represented in the MATLAB program. The start is from the substation, which contains the 33 kV supply source and related measuring devices, and enters the 33/11 kV transformer. Then the measuring instruments related to the voltage of 11 kV in addition over the current relay were represented. The measuring devices on the voltage of 11 kV include voltage and current gauges and symmetrical components for current in addition to the neutral current. The second stage is the representation of distribution transformers for their different capacities, and colors are used to distinguish these capacities. Finally, at the end of the feeder, measuring devices were placed similar to those found in the station. Figure 9 explains the Simulink design of the feeder f_4.

Do ten cases of load side broke conductor faults in every feeder.

5. Results and Discussion

5.1 Relationship Between Mathematical and Simulation Results

In the mathematical analysis, Equations (5) was used to determine the ground current $\left|I_g\right|_{mathmatical}$ from the sequence currents (I_0), (I_1), and (I_2) measured by the Simulink program in the substation side ($\bar{I}_{c1}$, $\bar{I}_{c2}$, and $\bar{I}_{c0}$) and Load side ($\bar{\bar{I}}_{c1,}$ $\bar{\bar{I}}_{c2}$, and $\bar{\bar{I}}_{c0}$) when the fault occurs in phase c. For example, take the measurements of the Fault Location (FL) in (0) position, as explained in Figure 10.

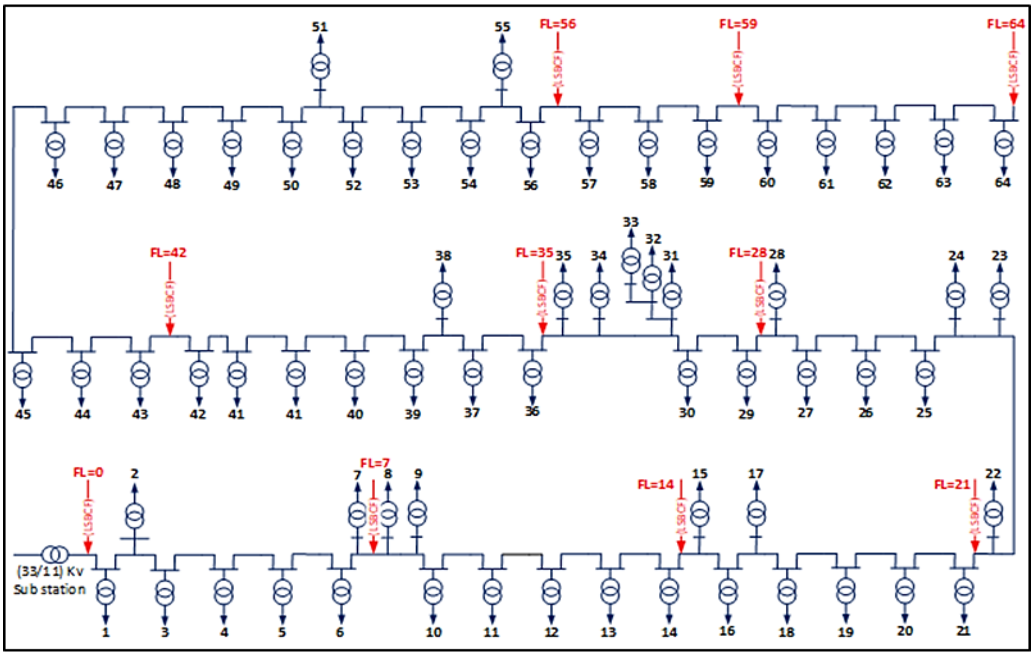

Figure 10: Fault locations to f_4

The results of the simulation are explained in Table 2. And then use equation 5 to determine $\left|I_g\right|_{mathmatical}$. As following:

Table 2: Comparison between simulation and mathematical result

Source side BCF (simulation result)			Load side BCF (simulation result)			Simulation	Mathematical	FL
$\overline{I}_{c1\,(A)}$	$\overline{I}_{c2\,(A)}$	$\overline{I}_{c0\,(A)}$	$\overline{\overline{I}}_{c1\,(A)}$	$\overline{\overline{I}}_{c2\,(A)}$	$\overline{\overline{I}}_{c0\,(A)}$	$\lvert Ig_{(A)}\rvert$	$\lvert Ig_{(A)}\rvert$	
186.2∟20.59	148.9∟80.41	37.3∟-38.67	223.5∟20.68	111.6∟80.17	0.139∟59.2	111.9	111.9	0
165.6∟19.9	132.7∟79.77	32.86∟-39.54	198.5∟19.96	99.87∟79.61	0.121∟56.42	98.59	98.7	7
146∟19.24	117.1∟79.1	29 ∟-40.27	175∟19.28	88.11∟79	0.115∟55.7	86.83	87	14
128.7∟18.65	103.4∟78.57	25.34∟-41.01	154.1∟18.67	78.01∟78.51	0.097∟53.41	76.04	76.4	21
109.7∟18.15	88.18∟78.11	21∟-41.67	131.2∟18.15	66.67∟78.1	0.073∟51.15	64.53	64.5	28
90.79∟17.81	72.96∟77.79	17.84∟-42.11	108.6∟17.8	55.12∟77.82	0.056∟50.18	53.53	53.43	35
69.34∟17.55	55.68∟77.55	13.66∟-42.45	83∟17.52	42.02∟77.61	0.045∟49.22	41	40.98	42
29.55∟17.15	23.68∟77.16	5.87∟-42.88	35.42∟17.11	17.81∟77.23	0.02∟48.16	17.62	17.61	56
19.7∟17.12	15.77∟77.11	3.922∟-42.84	23.62∟17.08	11.85∟77.18	0.018∟48.14	11.78	11.76	59
4.462∟17.01	3.571∟76.94	0.891∟-42.71	5.354∟16.97	2.679∟77	0.008∟48.12	2.677	2.676	64

$$\begin{bmatrix} Ig_{c0} \\ Ig_{c1} \\ Ig_{c2} \end{bmatrix}_{\text{Mathematically}} = 3\begin{bmatrix} 37.3\llcorner\text{-}38.67 - 0.139\llcorner 59.2 \\ 186.2\llcorner 20.59 - 223.5\llcorner 20.68 \\ 148.9\llcorner 80.41 - 111.6\llcorner 80.17 \end{bmatrix} = \begin{bmatrix} 111.9\llcorner 141.3 \\ 111.9\llcorner -158.9 \\ 111.9\llcorner 81.13 \end{bmatrix} \tag{11}$$

The results from Equation (11) are equal to those measured directly using the MATLAB program. As the following equations: -

$$\begin{bmatrix} Ig_{c0} \\ Ig_{c1} \\ Ig_{c2} \end{bmatrix}_{\text{Simulation}} = \begin{bmatrix} 111.9\llcorner 141.3 \\ 111.9\llcorner -158.9 \\ 111.9\llcorner 81.13 \end{bmatrix} \tag{12}$$

This means:

$$\left|I_g\right|_{mathmatical} = \left|I_g\right|_{simulation} \tag{13}$$

5.2 Results of Case Study F_1

A radial feeder f_1 is one of twelve feeders of Al- Abasia substation. The total number of distribution transformers is 15, as shown in Figure 11. The specification of f_1 covers design, manufacture testing, and inspection at the manufacturer's works of 11 kV high tension overhead feeder 11 kV, three-phase, 50 Hz, AC system. Table 3 shows the specifications and data used to perform the simulation f_1.

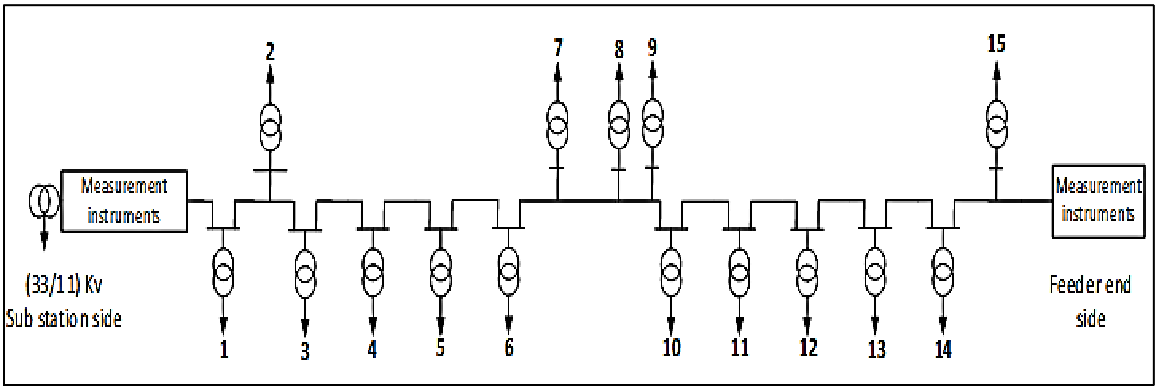

Figure 11: Case study test system of feeder f_1

Table 3: Specifications and data to f_1

Description	Value
Number of transformers	15
Length of 11kV feeder	4 km
Loads on the feeder	1420 kW
The distribution transformers rated power	(400, 250, and 100) kVA
The power transformer voltage level	(33/11) kV
Frequency rated	50 Hz
Distribution system transformers vector group	Dyn11
The distribution transformers voltage level	(11/0.4) kV
Rated power of power transformers	(2 x 31.5) MVA
The distribution feeder type	3-wire 3-phase
The conductor reactance	0.2899 ohm/km
The conductor resistance	0.246 ohm/km
The conductor type	120/20 mm^2 ACSR

A small sample of the feeders' number includes in Table 4, but it is comprehensive for the electrical network in terms of its difference in length, the number of transformers, etc. But the most important thing is that most loads of other electrical network feeders fall within the range of this table. Thus the limits of the problem and its solutions can be estimated, which is highly dependent on loads. Figure 12 illustrates a single-line diagram, where measurements are obtained at the substation for each of the ten cases of LSBC faults, and the results are as in Table 5.

Table 4: The specification of f1, f2, f3, and f4

Loads on the feeder	Length of 11kV feeder	Number of transformers	Feeder 11kV
1420 kW	4 km	15	f_1
2710 kW	6.5 km	30	f_2
4210 kW	8.1 km	47	f_3
6140 kW	11.1 km	64	f_4

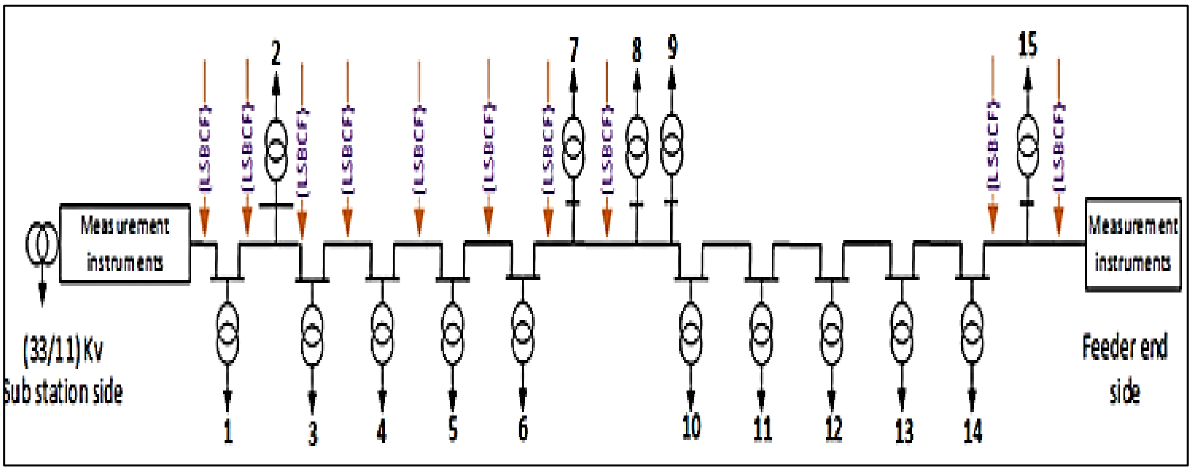

Figure 12: Implement ten LSBC faults for f_1

Table 5: The results at two feeder ends

Substation			Sub Station	Sub station	Sub station	Sub station	Sub station	Feeder end	Feeder end	Feeder end	Fault location
I_a (A)	I_b (A)	I_c (A)	I_{unb}%	I_n (A)	V_{ab} kV	V_{bc} kV	V_{ca} kV	V_{ab} kV	V_{bc} kV	V_{ca} kV	
76	76	0	100	29	11	10.98	11.02	10.99	6.336	6.353	0
77	76	5	93	27	11	10.98	11.02	10.99	6.335	6.350	1
77	77	11	86	25	11	10.98	11.02	10.99	6.336	6.349	2
77	77	16	79	23	11	10.98	11.01	10.99	6.336	6.348	3
78	78	21	73	22	11	10.98	11.01	10.99	6.337	6.346	4
78	78	27	65	20	11	10.98	11.01	10.99	6.337	6.345	5
79	79	32	59	18	11	10.99	11.01	10.99	6.337	6.345	6
80	79	37	53	16	11	10.99	11.01	10.99	6.338	6.345	7
84	84	73	13	4	11	10.99	11	10.99	6.342	6.344	14
85	85	78	8	3	11	10.99	11	10.99	6.343	6.344	15

5.2.1 Unbalance fault current detection

When the fault location is at the beginning of the feeder, it is noted in the phase current station columns in Table 5 that the values of the currents in un faulted phases drop from 86 amperes to 76 amperes. Still, in the faulty phase, its value is zero since the LSBC fault is present, as shown in Figure 13.

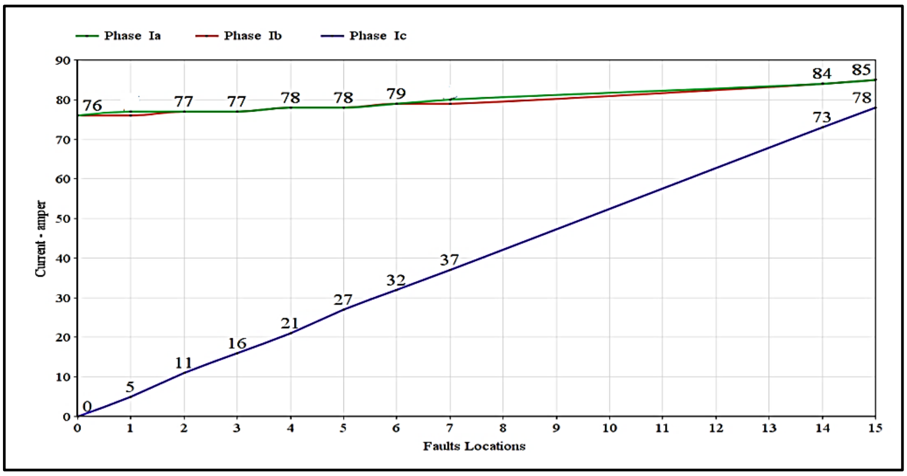

Figure 13: Unbalance three phase currents of f_1

When an LSBC fault is located distant from the sub-station, the current values in the defective phase grow until the threshold value is achieved. The threshold value is known as the magnitude that limits a change in the current value to less than 10%. Less than ten percent is the permitted amount in Iraqi electrical distribution systems. Therefore, the protection devices must protect the lines, as seen in Figure 14, if the percentage exceeds this threshold, which is considered a fault.

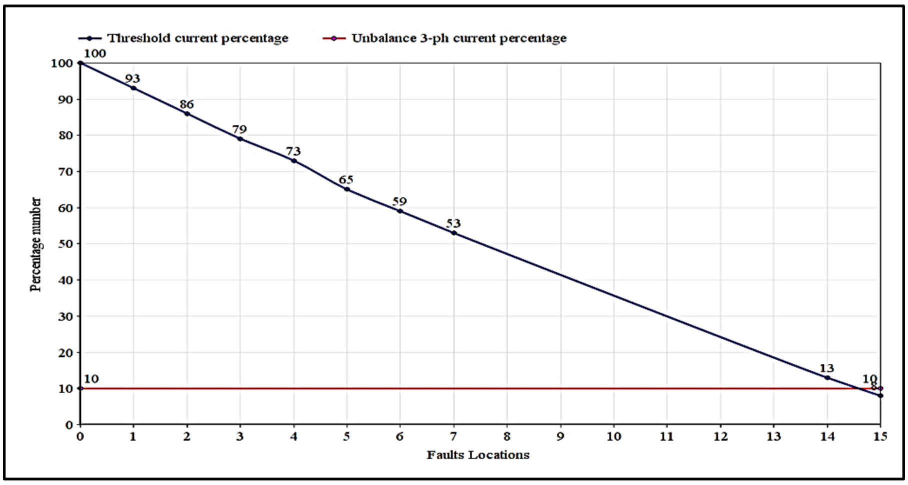

Figure 14: Unbalance 3-ph current percentage

Over-current protection cannot detect phase current into LSBC faults because of the permissible limits (300-750) A in Iraqi sub-stations. In this scenario, an imbalanced protection system can cover 90% of the 11 kV feeder. As a result, it can be stated that 90 percent of the feeder (Transformer number) can be kept secure by employing an unbalance phase current protection system.

The following aspects may be summarized from the above:

- According to the Iraqi standard, the allowable limit for imbalance 3-ph currents is less than 10%.
- An unbalance phase current protection system can cover 90% of the feeder.
- The disadvantage of the imbalance protection approach is that only 10% of the feeder is unprotected.

5.2.2 Neutral fault protection

Because the neutral current in Al-Abasia sub-stations was less than the permitted level of 40A, earth fault protection could not detect it. Therefore, equations (8) and (9) were used to calculate the range of current levels (30 to 150 amperes) over which the neutral protection functions (9).

When the current transformer (CT) is within the range permitted in Iraqi substations, which is 5/300, the constraints in Equations (8) and (9) apply. However, because the CT used in this case (Al-Abasia - 33/11 kV) is 5/400, the current values used by the protective devices will range (from 40 to 200) A. As a result of the fault current not being detected, the issue will worsen. The current levels in neutral in the ten LSBC fault cases in Table 5 ranged from (3-29) A, demonstrating that the protective devices are not responsive to the fault.

5.3 Case Study Test System Of F1 F2, F3, F4. for Unbalanced Current's Fault

Four 11kV feeders will be taken to be as a case for study. The data of each design and the event models are presented in Figure 15.

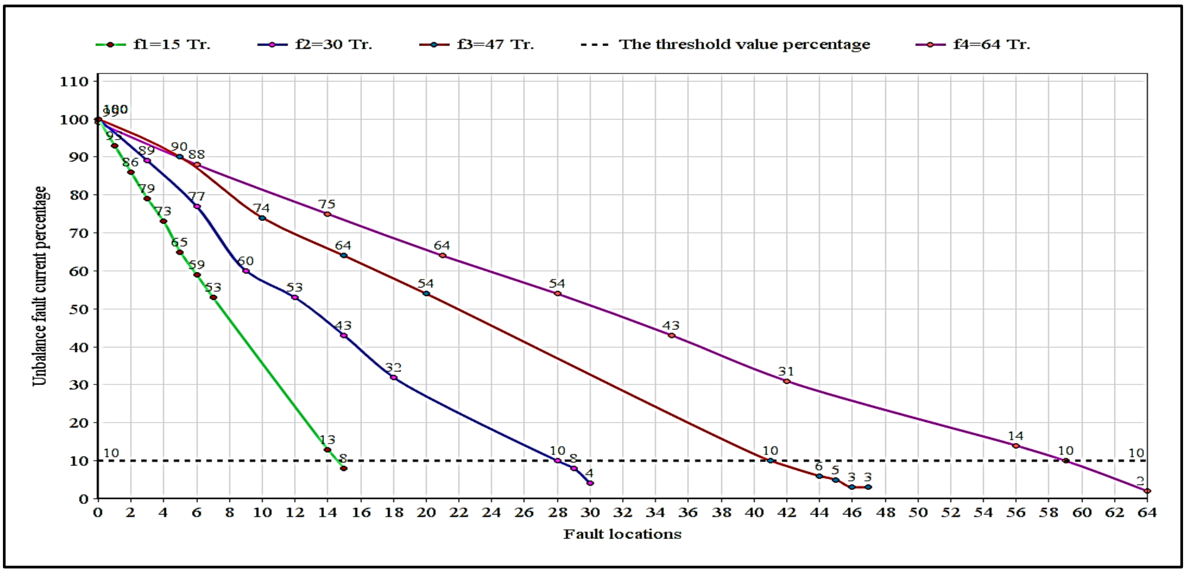

Figure 15: The unbalanced currents fault percentage to four feeders

As can be seen in Figure 15, the four feeders f_1, f_2, f_3, and f_4 differ among themselves in their values of reaching the threshold value of 10%, and more clearly in Table 6, the sensitivity ratios by the method of unbalanced currents of the four nutrients range from 87% to 93%.

Table 6: The total result of LSBC fault detection on the fourth feeder

Case study test system	Total number of transformers in the feeder	Threshold unbalanced current percentage value	Number of Tr. Where LSBC fault exceeds the threshold value	Unbalance current detection percentage of feeder Tr.
f_1	15	10%	14	93%
f_2.	30	10%	28	93%
f_3	47	10%	41	87%
f_4	64	10%	59	92%

5.4 Case Study Test System of F_1 F_2, F_3, F_4. for Neutral Fault Current

With the capacity to carry any fault current, neutral transformer grounding acts as a constant and permanent conductive connection to "earth". The amount of float depends mainly on the load balancing of the connected system and can be particularly damaging to single-phase loads.

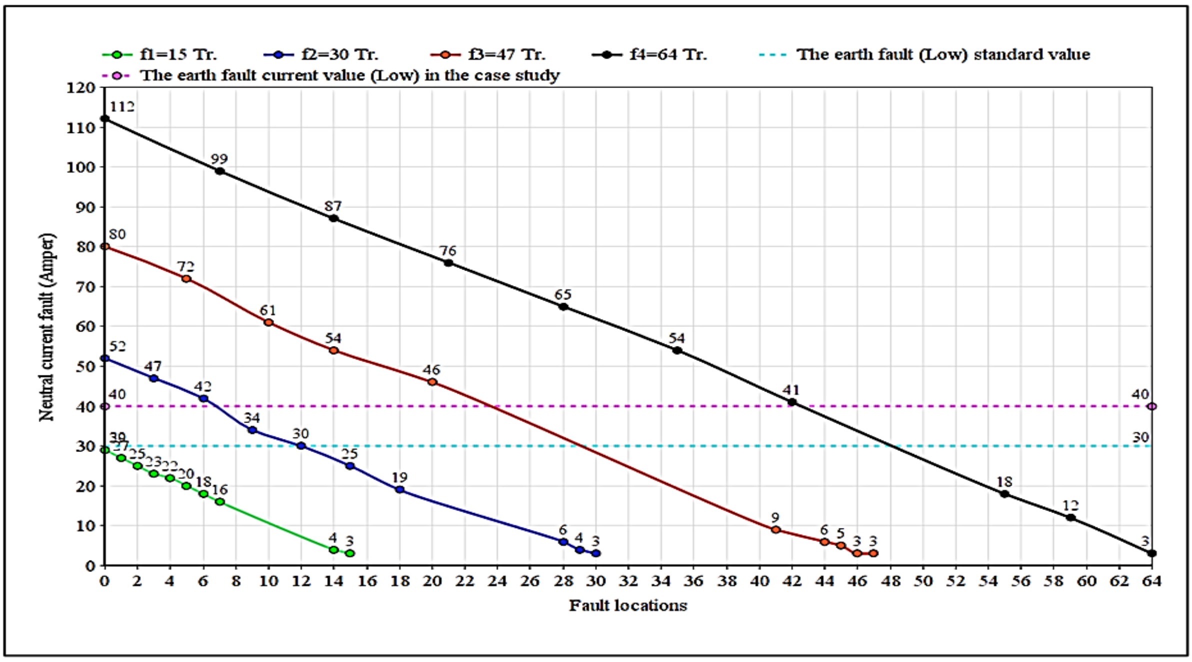

Figure 16: The neutral fault currents to four feeders

When a malfunction occurs, the neutral current that passes through the power transformer does not depend on the load balance but depends on two factors, namely the amount of load in the feeder and the distance of the fault from the station. We noticed from Figure 16 that the feeder f_4 is the highest load as it contains a higher number of transformers than the rest of the feeders f_1, f_2, and f_3, so the neutral current levels are higher than the rest of the feeders. As for the second factor, we note that the values of the neutral current are (110,80,53,30) amperes near the secondary station, and as the fault moves away from the station, these values begin to decrease.

Table 7: The total result of LSBC fault detection on the fourth feeder's neutral fault

Case study test system	Total number of transformers in the feeder	Neutral fault current protection percentage in (low) stander 30 A	Neutral fault current protection percentage in (low) stander 40 A.	Maximum neutral fault current (A)
f_1	15	0%	0%	30
f_2	30	40%	23%	53
f_3	47	61%	44%	80
f_4	64	70%	65%	110

In Table 7, the following points can be noted:

- When LSBC faults occur, the protection on the power transformer neutral is generally weak. In the best conditions, the safety of the nutrient does not exceed 70%. It distinguishes this type of malfunction from the rest of the malfunctions.

- As noted in the table, increasing the relay adjustment by ten amps leads to a decrease in the insured area of the neutral fault by a rate ranging between (15-23) %.
- Increasing the loads on the feeder is offset by an increase in the earth's fault currents. It thus causes an increase in the possibility of sensing the protection devices arranged in the transformer neutrals.
- Decreased load sometimes leads to the insensitivity of earth fault protection devices by 0%, as shown in f_1.

6. A Comparison between the Suggested Approach with Current Research

As mentioned in the literature, several methods have high accuracy, even better than the proposed method. For instance, the protection of 100% feeder loads and fault location is available, as fault detection. By contrast, in Table 8. the authors compare more advantages of their method with those of previous studies.

Table 8: A comparison of the suggested approach with recent research

The Proposed Technique	Methods used in the literature
• Using only measurements at the substation.	Using phase measurement unit data inside the substation and along with the feeders.[23], [7].
• Easy detection scheme (only measurement unit device)	Complex detection scheme (consisting of circuit intelligent electronic devices with phasor measurement unit data and Ethernet radio communication.) [24],[4]
• Detection of any Distribution Systems type (radial, ring, parallel, and interconnected) by Unbalanced Current Measurement	Detection of 11kV Ring Circuits by Unbalanced Current Measurement only [25],[9].
• It does not depend on arcing current.	Depending on the arcing current flow in the affected phase. Arc current does not occur in some cases when damaged conductors do not make contact. Thus, the detection method is incorrect. [26]
• Not depending on the communication system	requires a sophisticated communication link between the sensors and a significant, long-time delay for the signal transmission. [27]

7. Conclusion

The LSBC fault poses a serious risk to public security since the dropped line is not de-energized. It's a specialized type of single line to ground fault. It has a completely different effect on feeder current imbalance than a usual another fault since it happens on the LSBC fault. Therefore, the results confirmed that the over-current relay protection percentage in the Iraqi secondary stations 33/11kV is 0%. This is because the earth fault protection relay does not reach the pickup value for the low, neutral current of the LSBC fault. So, for neutral current fault protection at its best, it protects (0-70%) of the feeder 11kV. As can be seen, the LSBC fault detection scheme based on the unbalance 3-ph current is described for the problem solution in this paper. Additionally, the technical basis for this method is accessible. Nevertheless, the best solution that can be applied in the Iraqi distribution networks is the method of protection through unbalanced currents in substation (33/11) kV, where the protection ratios for 11 kV feeders are (87-93) % of its transformers. Still, the only drawback is that it does not protect the entire line. This protection electrical distribution network also benefits from compatibility with existing measurement equipment, even with the over-current relay in the electrical substation.

In comparison to earlier studies, the article has several advantages. Firstly, the detection of any distribution systems type (radial, ring, parallel, and interconnected) by Unbalanced Current Measurement. Secondly, the proposed method uses only measurements at the substation. Thirdly, this method did not depend on arcing current or the communication system.

On the other hand, several ideas and suggestions came up throughout this work, and they are worth pursuing to improve the distribution system management and operation. These suggestions may be summarized as follows:

1) Use the developed models to study and analyze the LSBC fault conductor localization.
2) Studying the limits and ratios of unbalance protection in practice for various forms of the electrical network, such as radial ring, parallel, and interconnected.
3) Implementing the proposed unbalanced 3-ph current digital relay setting method practically on Iraqi sub-station (33/11) kV.
4) Unbalance 3-ph current relay setting study and other studying like source side and open two sides broken conductor faults.

Author contribution

All authors contributed equally to this work.

Funding

This research received no specific grant from any funding agency in the public, commercial, or not-for-profit sectors.

Data availability statement

The data that support the findings of this study are available on request from the corresponding author.

Conflicts of interest

The authors declare that there is no conflict of interest.

References

[1] R. M. Carrie, K. Cheung, and K. Malik, Alternative approaches and dynamic analysis considerations for detecting open phase conductors in three-phase power systems, Electr. Power Syst. Res., 163 (2018) 59–65. https://doi.org/10.1016/j.epsr.2018.05.012

[2] A. C. Adewole, A. Rajapaksea, D. Ouelletteb, P. Forsythb, Residual current-based method for open phase detection in radial and multisource power systems, Int. J. Electr. Power Energy Syst., 117 (2020) 105610. https://doi.org/10.1016/j.ijepes.2019.105610

[3] D. K. Jayamaha, I. H. Madhushani, R.S. Gamage, P. P. B. Tennakoon, J. R. Lucas, U. Jayatunga, Open Conductor Fault Detection, 2017 Moratuwa Engineering Research Conference (MERCon), Moratuwa, Sri Lanka, 2017, 363-367. https://doi.org/10.1109/MERCon.2017.7980511

[4] J. Li, H. Loehner, T. Doshi, Detecting and Isolating Falling Conductors in Midair Using 900 MHz Private LTE at Protection Speeds, Schweitzer Engineering Laboratories, Inc.2022.

[5] E. M. Esmaila, M. M. Elgamasy, T. M. Kawada, A. M. Taalab, N. Elkalashy, and M. A. Elsadd, Detection and experimental investigation of open conductor and single-phase earth return faults in distribution systems, International Int. J. Electr. Power Energy Syst., 140 (2022) 108089. https://doi.org/10.1016/j.ijepes.2022.108089

[6] Y. Du, W. Tan, Power Based Open Phase Condition Detection Scheme, IOP Conf. Ser.: Earth Environ. Sci., 632,2021, 042012. https://doi.org/10.1088/1755-1315/632/4/042012

[7] S. V. Fernandes, D. V. Jo˜ao, M. A. I. Martins, H. G. B. Souza, A. F. Macedo, and K.A. Martins, A Symmetrical Component Evaluation for Broken Conductor Fault Detection, 2021 6th International Conference for Convergence in Technology (I2CT), Maharashtra, India, 2021, 1-6. https://doi.org/10.1109/I2CT51068.2021.9417933

[8] M. A. Dilli, H. M. A. Nascimento, J. C. Silva, Conductor break detection in distribution system through negative sequence voltage, RIELAC, Septiembre-Diciembre, 42 3 (2021) 31-44.

[9] X. Wang, and W. Xu, A 3rd harmonic power based open conductor detection scheme, IEEE Transactions on Power Delivery, 36 (2021) 1041-1050. https://doi.org/10.1109/TPWRD.2020.3001075

[10] J. S. Hong, S. Y. Hyun, Y.W. Lee, J. H. Cohi, S. J. Ahn, A. S. Y. Yun, Detection of Open Conductor Fault Using Multiple Measurement Factors of Feeder RTUs in Power Distribution Networks with DGs, In IEEE Access, 9 (2021) 143564-143579. https://doi.org/10.1109/ACCESS.2021.3121880

[11] A. Wontroba, A. P. Morais, G. J. Cardoso, J. P. A. Vieira, P. E. Farias, M. Gallas, J. P. Rossini, High-Impedance Fault Detection on Downed Conductor in Overhead Distribution Networks, Electr. Power Syst. Res., 211 (2022) 108216. https://doi.org/10.1016/j.epsr.2022.108216

[12] S. Aarsey, A. Bhargav, Review Paper on Single and Three Phase Fault Identification System using Machine Learning, Int. J. Res. Publ. Rev., 3 (2022) 54-60.

[13] H. Mirshekali, R. Dashti, A. Keshavarz, and H. R. Shaker, Machine Learning-Based Fault Location for Smart Distribution Networks Equipped with Micro-PMU, MDPI, Basel, Switzerland, Sensors, 2022. https://doi.org/10.3390/s22030945

[14] M. Bhatnagar, and A. Yadav, Fuzzy based relaying scheme for high impedance faults in DG integrated distribution system, Electr. Power Syst. Res., 202 (2022) 107602. https://doi.org/10.1016/j.epsr.2021.107602

[15] A.G. Al-Baghdadi, M. K. Abd, F. M. F. Flaih, A New Detection Method for Load Side Broken Conductor Fault Based on Negative to Positive Current Sequence, Electronics, 11, 2022,836. https://doi.org/10.3390/electronics11060836

[16] K. Ma, L. Fang, and W. Kong, Review of distribution network phase unbalance Scale, causes, consequences, solutions, and future research directions, CSEE J. Power Energy Syst., 6 (2020) 479-488. https://doi.org/10.17775/CSEEJPES.2019.03280

[17] H. K. Wong, S. Chen, S. Lau, J. Tang, K. P. Liu, Detection of Open-circuit Fault in 11kV Ring Circuits by Unbalanced Current Measurement, 2006 IEEE PES Power Systems Conference and Exposition, 2006,1240-1243. https://doi.org/10.1109/PSCE.2006.296484

[18] J. Pan, J. Liu, X. Chen, K. Zhong, Three-phase unbalanced load control based on load–electricity transfer index, Energy Rep.,7 (2021) 312-318. https://doi.org/10.1016/j.egyr.2021.01.064

[19] M. Bina, and A. Kashefi, Three-phase unbalance of distribution systems: Complementary analysis and experimental case study, Int. J. Electr. Power Energy Syst., 33 (2011) 817-826. https://doi.org/10.1016/j.ijepes.2010.12.003

[20] The republic of Iraq ministry of electricity (MoE), Energy distribution office, Construction of 33/11kV Substations (2 x 31.5 MVA) Section (1), Technical specifications.

[21] J. M. Gers, E. J. Holmes, Protection of Electricity Distribution Networks, 3rd Edition, Inst.Eng. Technol., Power and Energy Series, 2011.

[22] https://www.garmin.pk/oregon-750.html

[23] A. Marquez, A. Torres, I. Sanchez, K. Tran, M. Webster, Y. Yin, G. G. Solutions, High-Speed Falling Conductor Protection in Distribution Systems using Synchro phasor Data, Alfredo Marquez, Arturo Torres, Ignacio Sanchez, Kiet Tran, and Matthew Webster Southern California Edison Company, USA,2022.

[24] W. O'Brien, E. Udren, K. Garg, D. Haes and B. Sridharan, Catching falling conductors in midair detecting and tripping broken distribution circuit conductors at protection speeds, 2016 69th Annual Conference for Protective Relay Engineers (CPRE), College Station, TX, USA, 2016, 1-11. https://doi.org/10.1109/CPRE.2016.7914881

[25] H. K. Wong, S. Chen, S. K. Lau, J. Tang and K. P. Liu, Detection of Open-circuit Fault in 11kV Ring Circuits by Unbalanced Current Measurement, 2006 IEEE PES Power Systems Conference and Exposition, 2006,2006, 1240-1243. https://doi.org/10.1109/PSCE.2006.296484

[26] L. Himadri, K. Subrata, Classification of arc fault between broken conductor and high-impedance surface: an empirical mode decomposition and Stockwell transform-based approach, IET Gener. Transm. Distrib., Inst.Eng. Technol., 14 (2020) 5277-5286 .

[27] E. Bjerkan, H. K. Høidalen, J. G. Hernes, N. E. T. AS-Norway, Reliable detection of downed and broken conductors,In CIRED 19th International Conference on Electricity Distribution, 2007,1-4.

Appendix

Appendix. Datasheet for f_{10} / 11kV**.**

Sub-Station: محطة العباسية　　Page of: 1　　Feeder Distence: 4 km
Feeder No.: F10　　Date:　　No. of Poles:
Feeder Name: الوهابي　　Last UpDate: 17/5/2012

Start Point	Distence (M)	No. of Poles	Next Point	Conductor Type	Transformer (KVA)	Transformer Position	Switch	Type of Consumers	position	Notes
Station	11		1	UG					N32 09.037 E44 26.368	
1	60		2	UG					N32 09.030 E44 26.394	
2	332		3	UG					N32 09.024 E44 26.332	
3	145		4	UG					N32 09.016 E44 29.043	مقابل مركز شرطة المرور
4	10		5	UG					N32 08.974 E44 26.610	
5	15		6	UG					N32 08.971 E44 26.164	
6	20		7	UG					N32 08.947 E44 28.955	
7	57		8	UG					N32 08.939 E44 26.083	مقابل مصرف الرافدين
8	6		9	UG					N32 08.935 E44 28.940	
9	155		10	UG					N32 08.928 E44 26.087	
10	5	1	11	UG					N32 08.914 E44 25.943	رأس كيبل المغذي
11	226	6	12	Al 120	250KVA	Outdoor		Residential	N32 08.908 E44 25.943	
12	78	2	13	Al 120					N32 08.900 E44 26.953	
13	32	2	14	Al 120	250KVA	Outdoor		Government	N32 08.899 E44 26.957	محولة مشروع ماء الخوية
13	210	5	15	Al 120					N32 08.898 E44 26.940	
15	216	4	16	Al 120					N32 08.883 E44 25.849	
16	35	2	17	Al 120	250KVA	Outdoor		Residential	N32 08.876 E44 25.810	مقابل محل للغذائية
17	219	5	18	Al 120					N32 08.875 E44 26.919	
18	41	1	19	Al 120					N32 08.867 E44 25.775	
19	318	7	20	Al 120	250KVA	Outdoor		Residential	N32 08.866 E44 25.868	
20	476	9	21	Al 120					N32 08.857 E44 25.824	
21	43	2	22	Cu 50	250KVA	Outdoor		Agriculture	N32 08.842 E44 25.771	
22	324	7	23	Al 120	100KVA	Outdoor		Agriculture	N32 08.840 E44 25.671	بيت ابو صالح عبد الزهره
23	22	2	24	Al 70	250KVA	Outdoor		Agriculture	N32 08.837 E44 25.672	محولة سيد هاتف المحنة
23	24	2	25	Al 70	250KVA	Outdoor		Agriculture	N32 08.834 E44 28.257	
23	24	1	26	Al 120					N32 08.829 E44 28.780	
26	236	5	27	Al 120					N32 08.816 E44 28.275	
27	29	2	28	Al 120	250KVA	Outdoor		Government	N32 08.782 E44 27.359	مشروع ماء الاعمى
28	11	1	29	Al 120					N32 08.765 E44 27.350	
27	83	3	30	Al 120	400KVA	Outdoor		Residential	N32 08.764 E44 25.535	حسينية سيد موسى
30	49	1	31	Al 120					N32 08.761 E44 28.049	
31	103	4	32	Al 120	250KVA	Outdoor		Residential	N32 08.759 E44 28.021	مقابل بيت علي جاسم
32	79	2	33	Cu 50					N32 08.756 E44 28.253	

Note 1: For the transformer position: Indoor (I), Outdoor (O), Kiosk (K)

Note 2: Type of consumers: Residential (R), Commercial (C), Industrial (I), Agriculture (A), Government (G), etc. If the transformer is shared for example, Industrial & Domestic enter as Ind/Dom

برامجيات تخطيط الشبكات 2020